

Optical Analysis of Potential Well Resonances*

K. W. McVOY†

University of Wisconsin, Madison, Wisconsin

L. HELLER

Los Alamos Scientific Laboratory, Los Alamos, New Mexico

M. BOLSTERLI‡

University of Minnesota, Minneapolis, Minnesota

As a contribution toward the understanding of resonant scattering in general, we examine the potential-barrier resonances which occur in a variety of simple one- and two-channel S -wave scattering problems. The models chosen have familiar optical analogs which, together with the appealingly simple analytic properties of their scattering amplitudes, facilitate a unified discussion of such diverse phenomena as the peculiar S -wave “resonances” of a square potential well, the occurrence of “resonance circles” in both elastic and inelastic scattering amplitudes, and the large nonresonant maxima which the descent of the background phase (as a function of energy) can produce in total cross sections.

I. INTRODUCTION

Because each branch of physics tends to develop its own personal nomenclature, it is not uncommon for the same physical phenomenon to occur in two or more fields under entirely different names. Standing-wave resonances provide a particularly striking example, and it has long been recognized that the potential-barrier resonances¹ of scattering theory, the transmission maxima of a Fabry-Perot interferometer (band-pass filter), and the appearance of standing waves in waveguides, transmission lines, and musical instruments are all manifestations of the same cavity-resonator principle. Our purpose in revisiting them here is threefold. First, by examining mathematically simple models of such a resonator, it is possible to exhibit in direct and appealing fashion the complex-energy poles of the corresponding scattering amplitude (transfer or response function in optical or circuitry terms) which are “responsible” for the resonance peaks the function exhibits at nearby real energies.² Second, these same models show explicitly how the sharpness of these resonances depends on the reflection coefficient of the cavity walls, and so explain why a potential well with a barrier at its edge can have narrow resonances (below the top of the barrier) whereas the poles for S -wave scattering by a well without a barrier hardly produce resonances at all. Third, if the cavity (of linear dimension R) is highly reflecting to waves incident upon it from the outside, the non-resonant part of the phase shift which it induces in the reflected waves will show a “hard-sphere” type of energy dependence, $\delta_{n,r} \sim -kR$, a descending back-

ground phase shift which can cause broad “echo” maxima in the scattering cross section at energies between resonances.³⁻⁶ Consequently, if such a resonator is coupled to two open channels, it provides a particularly clear example of the way in which these non-resonant echoes come to dominate the total cross section if the resonance is gradually decoupled from the entrance channel.

Because our primary concern is with resonance phenomena—including unusual examples such as those of the square well—it is important to have a universal and unambiguous definition of what we mean by the (real) energy—or equivalently momentum—of a resonance. A particularly helpful feature of the cases we consider is that the “optical” approach provides expressions for all S -matrix elements, as well as for the amplitude of the internal or trapped wave, in N/D form, with the same $D(k)$ function (the Jost function in one-channel cases) occurring throughout a given problem. From a theorist’s viewpoint the zeros, $k_n = k_{0n} - i\gamma_n$ of $D(k)$ in the complex-momentum plane provide the most natural definition of the (complex) momenta of the resonating states, in customary Breit-Wigner fashion. More physically, this suggests using $\text{Re}(k_n) = k_0$ as the *real* resonance momentum. In every case considered here, k_0 is very near those real momenta at which (a) the internal wave amplitude, $|A(k)|$, has a maximum, (b) the phase shift derivative $d\delta/dk$ (eigenphase if more than one channel is open) has a maximum, and (c) $|D(k)|$ has a minimum. Since these are all desirable attributes of a scattering resonance, we adopt this as our definition of resonance momentum throughout the present paper. Although for sufficiently low-energy resonances k_0 is also the momentum at which $\delta \cong \pi/2$, there is of course no reason for this to be true in general; practi-

* Work supported in part by U.S. Atomic Energy Commission and the National Science Foundation.

† These two authors wish to thank Dr. J. E. Young and Dr. J. C. Mark for the hospitality extended to them at the Los Alamos Scientific Laboratory during the summer of 1965.

¹ But not the “compound nucleus” type of resonance, which is best considered as an intermediate state in a closed channel, and is not dependent on a geometrical barrier for its long lifetime.

² Analogous analyticity properties are also discussed for similar models by K. T. R. Davies and M. Baranger, *Ann. Phys. (N.Y.)* **19**, 383 (1962).

³ J. M. Peterson, *Phys. Rev.* **125**, 955 (1962). See also S. Fernbach and R. Serber, and T. B. Taylor, *Phys. Rev.* **75**, 1352 (1949).

⁴ K. W. McVoy, *Phys. Rev. Letters* **17**, 42 (1965).

⁵ M. Born and E. Wolf, *Principles of Optics* (The Macmillan Co., New York, 1959), p. 662, Fig. 13.14.

⁶ H. C. van de Hulst, *Light Scattering by Small Particles* (John Wiley & Sons, Inc., New York, 1957), p. 177.

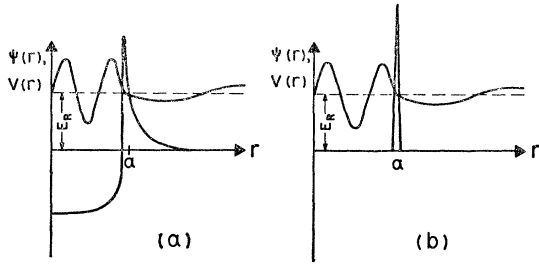


FIG. 1. (a) Potential well and surface barrier, with wave function at a resonant energy. Note sharp bend of the wave function inside the barrier. (b) Delta-function potential, showing break in slope of the wave function at $r=a$.

cally speaking, a resonance appears as a sharp change in the energy dependence of a cross section, which may or may not occur at a maximum. Finally, by antiresonance we normally mean an energy at which the amplitude of the internal wave function has a minimum.

In Sec. II we discuss the scattering properties of a delta function potential barrier (partially silvered spherical shell) and in Sec. III generalize this to the two-channel case. Section IV considers the “resonant” properties of S -wave scattering by a square potential well (glass ball in air) and barrier (air bubble in glass), and Sec. V examines in detail the inelastic resonances of a particular two-channel resonator which is the scattering analogue of a Fabry-Perot etalon. To simplify the algebra we adopt, throughout, units in which $\hbar=c=1$.

II. ELASTIC S -WAVE RESONANCE

A. S -Matrix Element for a Thin Barrier

Perhaps the simplest example which exhibits resonances is the scattering of a train of ingoing S waves by a thin spherical shell whose center is at their center of symmetry. This is an idealization of S -wave scattering by the Schrödinger potential of Fig. 1(a) (often encountered in nuclear and molecular problems), which consists of a central attractive region surrounded by a repulsive barrier at $r \approx a$. If the central region is large enough to accommodate integral numbers of internal half-wavelengths, $K_n a = n\pi$, at energies below the top of the barrier, the energies E_n corresponding to K_n will be resonance energies, at which the phase shift rises rapidly with energy and $|\psi_{\text{int}}/\psi_{\text{ext}}|^2 \sim 1/T$, a number which can become arbitrarily large if the transmission coefficient T of the barrier is made small at E_n . From a wave optics point of view the barrier may be viewed as a thin spherical shell whose index of refraction is much lower than that of the surrounding medium. The two changes of velocity suffered by waves traveling outward through the barrier provide

the reflection necessary to trap them efficiently and permit the buildup of a resonant state. Equivalently, the barrier can be thought of as providing the high frequencies and short wavelengths present in the sharp bend the wave amplitude suffers where its large internal resonant amplitude joins the small external amplitude.

If this bend occurs over a finite distance, the essentials of the phenomenon become obscured by the details involving the exact height and shape of the barrier. A useful and familiar idealization is obtained by replacing the actual barrier by an infinitely thin shell, i.e., a delta-function potential, which bends the wave function sharply at a single radial distance. Although the inside attractive well is essential for bound states, it is unnecessary for resonances, so we dispense with it and take as our example a single delta-function potential, $2m V(r) = c\delta(r-a)$.

Such a potential (equivalent to two large velocity changes in rapid succession) will partly reflect and partly transmit any wave incident on it; optically it is a partly silvered mirror. Consequently, finding the radial wave function $u(r) = rR(r)$ of the S -wave scattering problem is equivalent to obtaining the standing-wave pattern established by waves incident normally from the right on a partly silvered mirror which is backed up by a perfect mirror [the node boundary condition $u(0) = 0$] at a distance a behind it, Fig. 1(b). This standing wave is readily found by the technique customarily used to analyze the Fabry-Perot interferometer. We find this approach more useful than simply solving the Schrödinger equation for a delta-function potential, not only because of the light it sheds on the resonance mechanism, but also because the important properties of the scattering amplitude are more readily extracted by writing it as a function of the reflection amplitude of the delta function, $\rho(c)$, rather than directly as a function of c itself.

By the reflection amplitude we mean the (generally complex) number ρ defined by the condition that the wave $\exp(-ikr)$ incident on a mirror at the origin produce the reflected wave $\rho \exp(ikr)$. If the reflection takes place at $r=a$, the outgoing wave must be $\rho \exp(-2ika) \exp(ikr)$ in order that

$$\rho[\exp(-2ika) \exp(ika)]/\exp(-ika)$$

will still be the ratio of reflected to incident amplitudes at the mirror; the extra factor $\exp(-2ika)$ clearly represents a reduction in phase accumulation due to a shortening of the optical path length by the round-trip distance $2a$.⁷ The reflection coefficient of the barrier, R , which tells what fraction of the incident particles is reflected, is $|\rho|^2$ for waves incident from either the left or right.

⁷ If the incident wave is $\exp(ikr)$, approaching the mirror from the left, the reflected wave is $\rho \exp(2ika) \exp(-ikr)$.

Provided the mirror does not have a dipole layer of "charge" on it [e.g., $V(r) = c\delta'(r-a)$], the wave amplitude must be continuous through it. If the incident wave $\exp(-ikr)$ produces the transmitted wave $\tau \exp(-ikr)$ this means

$$\tau \exp(-ika) = \exp(-ika) + \rho \exp(-2ika) \exp(ika)$$

or

$$\tau = 1 + \rho. \quad (1a)$$

This is the continuity condition. T , the transmission coefficient of the barrier, is defined to be the fraction of the incident particles which is transmitted; in this problem $T = |\tau|^2$. If in addition the mirror is non-absorptive, so that the flux or current of the wave system is continuous at $r=a$, the coefficients also satisfy the unitarity condition,⁸

$$|\tau|^2 + |\rho|^2 = T + R = 1, \quad (1b)$$

which together with (1a) implies

$$\rho + \rho^* + 2|\rho|^2 = 0. \quad (2)$$

This in turn is equivalent to

$$|1 + 2\rho| = 1, \quad (3)$$

i.e., the complex number ρ is restricted to lie on the circle of radius $\frac{1}{2}$ which is centered at $(-\frac{1}{2}, 0)$, Fig. 2. As $\rho \rightarrow -1$ along the circle, $\tau \rightarrow 0$ and the mirror becomes a perfect reflector. Of course if there is absorption, then $|\tau|^2 + |\rho|^2 < 1$; in that case $|1 + 2\rho| < 1$.

The reflection and transmission amplitudes for the delta function potential $2mV(r) = c\delta(r-a)$ are directly found to be

$$\rho(c, k) = \frac{-ic/2k}{1 + ic/2k},$$

and

$$\tau(c, k) = (1 + ic/2k)^{-1}, \quad (4)$$

which, of course, satisfy Eq. (1) (for real c and k). By way of orientation we note that ρ vanishes when c does, since no potential means no mirror, and $c \rightarrow \infty$

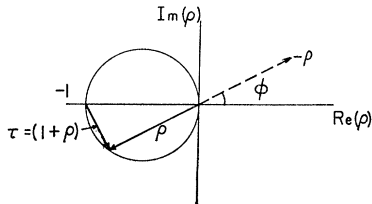
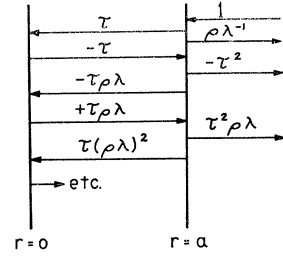


FIG. 2. Complex reflection amplitude ρ for the delta function potential of Fig. (1b), which lies on the circle $|\rho + \frac{1}{2}| = \frac{1}{2}$ if the potential is real. The transmission amplitude $\tau = 1 + \rho$ is also shown.

⁸ Equation (1b) is a general property of any nondissipative barrier, but (1a) is clearly a special characteristic of an infinitely thin one.

FIG. 3. Multiple internal reflections within the "thin film" formed by a perfect mirror ($\rho_0 = -1$) at $r=0$ and a partly silvered mirror (delta-function potential) at $r=a$. The incident wave is shown at the top approaching from the right with unit amplitude. The amplitudes of successive portions of the wave train are indicated after various numbers of reflections and transmissions. $\lambda = \exp(2ika)$.



implies $\rho \rightarrow -1$ or $\tau \rightarrow 0$; a potential this strong is a perfect mirror. ρ and ρ^* differ only in the sign of the potential (assuming c real); an attractive potential puts ρ in the upper half-plane. Because of the symmetry of the potential, the reflection amplitude is the same for waves incident from either the right or the left.

The steady-state scattering problem for a system composed of a mirror with amplitudes (ρ, τ) at $r=a$, and a perfect reflector $(-1, 0)$ at $r=0$ is readily solved in terms of ρ by the familiar method of following the infinitely long wave train through its successive transmissions and reflections, as indicated in Fig. 3. The essential feature of the solution is the "resonance series" of internally reflected amplitudes,

$$1 - \rho \exp(2ika) + [\rho \exp(2ika)]^2 - \dots = [1 + \rho \exp(2ika)]^{-1}, \quad (5)$$

in terms of which

$$u_{\text{int}}(r) = [\tau / (1 + \rho\lambda)] [\exp(-ikr) - \exp(ikr)] = -2i[\tau / (1 + \rho\lambda)] \sin kr, \quad r < a \quad (6a)$$

and

$$u_{\text{ext}}(r) = \exp(-ikr) + \{\rho\lambda^{-1} - [\tau^2 / (1 + \rho\lambda)]\} \exp(ikr) = -2ie^{i\delta} \sin(kr + \delta), \quad r > a \quad (6b)$$

where $\lambda(k) = \exp(2ika)$. With the Jost function $f(k) = 1 + \rho\tau^{-1}(1 - \lambda^{-1})$, the internal amplitude $A(k) \equiv \tau / (1 + \rho\lambda)$, is equal to $1/f(-k)$ provided ρ/τ is an odd function of k . This will be the case, for example, if the potential energy is independent of momentum.

The amplitude of the external outgoing wave is the reflection amplitude for the entire two-mirror system; its negative is called the S -matrix element for the S -wave scattering problem,

$$S(k) \equiv \exp(2i\delta) = -\rho\lambda^{-1} + [\tau^2 / (1 + \rho\lambda)] = (1 + 2\rho - \rho\lambda^{-1}) / (1 + \rho\lambda) \quad (7a)$$

$$= (1 + 2\rho) [(1 + \rho\lambda)^* / (1 + \rho\lambda)], \quad (7b)$$

where $\rho + \rho^* + 2|\rho|^2 = 0$ has been used to obtain (7b) which is valid only if c (and k) are real. For the remainder of this section we consider only this case, for

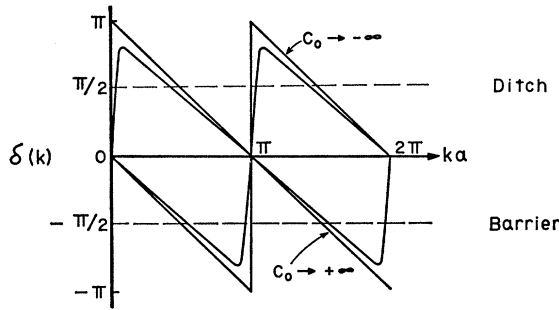


FIG. 4. Energy dependence of *S*-wave phase shifts for scattering by a momentum-dependent potential of the form $2mV(r) = c(k)\delta(r-a)$, with $c=c_0k$. The positive phase shift is for $c_0 < 0$ and the negative one for $c_0 > 0$. $c_0 \rightarrow \pm\infty$ gives the hard-sphere phase shift $\delta(k) = -ka \pmod{\pi}$, and $c_0 = 0$ gives $\delta(k) \equiv 0$. The intermediate curves shown are for $c_0 = \pm 7$.

which $A(k) = 1/f^*(k^*) = \exp(i\delta)/|f(k)|$. From this last form it is clear that $|S|^2 \equiv 1$, or the phase shift δ is real, as it must be for a nonabsorptive scatterer. We note that $S = +1$ ($\delta = 0$) whenever $\lambda = +1$ or $ka = n\pi$, a peculiarity of this model, due to the fact that the interaction is concentrated entirely at $r = a$, and causes no scattering if the wave pattern has a node there. The nonresonant term $-\rho \exp(-2ika)$ (due to the initial reflection of the incoming wave) is the only one to survive if $\rho \rightarrow -1$ and $\tau \rightarrow 0$; this makes the delta function a perfect mirror and so gives $\delta = -ka$.

The more detailed properties of $\delta(k)$ involve the energy dependence of ρ and would clearly be simplest if ρ were constant. This is the analog of a frequency-independent index of refraction. It is readily achieved if we are willing to admit a momentum-dependent potential strength, i.e., c proportional to k , so that the transmission coefficient T , which normally approaches 1 at high energy, is instead held constant. In the interest of simplicity we examine this case, and obtain the phase shifts of Fig. 4, which contain ρ simply as a

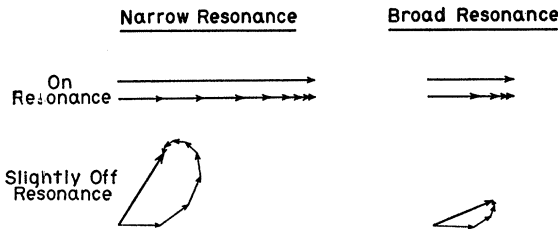


FIG. 5. Complex vector diagram indicating the addition of successive amplitudes of waves reflected internally from the walls of the thin film of Fig. 3. On resonance the ratio of successive amplitudes, a_{n+1}/a_n , is the real number $|\rho|$ which is nearly 1 for a narrow resonance (large sum) and $\ll 1$ for a broad resonance (small sum). Slightly off the resonance energy the ratio is still $|\rho|$ in absolute magnitude, but has a small phase. This causes the sum to decrease drastically from its on-resonance value because of destructive interference or "curling" in the narrow case, but it decreases very little in the broad case.

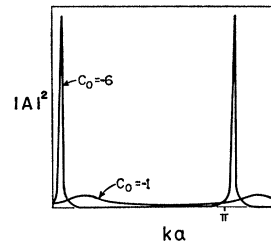


FIG. 6. Amplitude-squared of the internal wave function for the thin film of Fig. 3 as a function of bombarding energy, showing narrow resonances when the barrier is highly impenetrable ($c_0 = -6$) and broad ones when it is transparent ($c_0 = -1$).

constant parameter. They are periodic in ka in this case and vary between the extremes of the sawtooth shape obtained for $\rho = -1$ (perfect reflector) and $\delta(k) \equiv 0$ for $\rho = 0$.

The most significant property of this example is the set of sharp resonances which occur for ka slightly less than $n\pi$ (approximating the bound state condition of a node at $r = a$) if the barrier reflects strongly and transmits little. The fact that low transmission will yield a long resonance lifetime and hence a narrow emitted line follows from the uncertainty principle for an arbitrary resonator, but can be seen quite dramatically for cavity resonators from the traditional vector diagram of physical optics, Fig. 5, which follows graphically the summation of the resonance series of complex numbers (vectors), Eq. (5).

Although the summation of this series only affects the phase of the outgoing wave, it has a spectacular effect on the wave inside the cavity, whose amplitude

$$A(ka) = \tau / [1 + \rho \exp(2ika)] \quad (8)$$

can build up to an arbitrarily large value at a narrow resonance.

The k dependence of $|A(ka)|^2$, Fig. 6, is readily understood from Fig. 7, which shows how $|1 + \rho\lambda|$ oscillates as $\rho\lambda$ travels around a circle of radius $|\rho|$ and produces the amplitude

$$|A|_{\max} = |\tau| / (1 - |\rho|) = [|\tau| (1 + |\rho|)] / |\tau|^2 = (1 + |\rho|) / |\tau|, \quad (9)$$

in the resonance region. Mathematically this amplitude

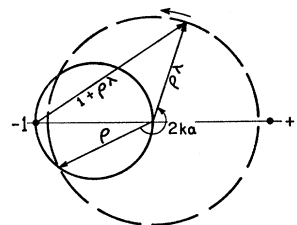


FIG. 7. The path followed in the complex plane by $\rho\lambda$ as the energy increases is shown as the dashed circle; the ρ circle of Fig. 2 is included for comparison. Note that the vector $[1 + \rho\lambda(k)]$, which is essentially the Jost function for the potential of Fig. 1b, becomes very small at resonance ($\rho\lambda$ real and negative) if $|\rho|$ is close to 1.

becomes large as $|\tau| \rightarrow 0$ because $|\rho| \rightarrow 1$ and the series (5) diverges. Physically, the successive terms of the series are the amplitudes of successive rays traveling in the same direction; at resonance ($\rho\lambda$ real and negative) they are in phase and add up to a very large number if successive terms are nearly the same size, which they can be only if the leakage out through the delta function mirror is small at each reflection. In the antiresonance region successive rays are out of phase and the sum of the series is small by cancellation (destructive interference). The phase-shift oscillations can also be followed in Fig. 7 by noting from Eq. (7) that $(1+\rho\lambda)$ is proportional to $\exp(-i\delta)$, so that its phase is $-\delta$ to within an additive constant.

Since one is accustomed in potential scattering theory to associating resonances with potential barriers, it is somewhat surprising to note from Eq. (9) and Fig. 4 that equally good resonances are obtained for $c > 0$ and $c < 0$ (ρ or ρ^*), i.e., for a potential barrier and a potential ditch. The only essential feature is the high reflection and low transmission of the double velocity change, which is provided as adequately by the "attractive" potential as by the "repulsive" one. As illustration, Fig. 8 shows wave functions for a highly reflecting ditch ($c < 0$), both at resonance [where $\delta(k)$ passes steeply upward through $\pi/2$] and at antiresonance [where $\delta(k)$ passes slowly downward through $\pi/2$].

The other significant feature of the phase shifts of Fig. 4 is their behavior between resonances, which is very like the phase shift due to a hard-sphere scatterer. This "background" phase shift comes largely from the first reflection of the wave from the outside of the sphere and so can be expected from any scatterer with a fairly strong external reflection coefficient. The momentum-spacing between resonances for this simple delta-function barrier is $\Delta(ka) = \pi$, which Fig. 4 shows to be enough to permit this hard-sphere effect to bring the phase shift down by just the amount of its rise at the preceding resonance. Consequently, if the resonance is strong enough to force the phase up through $\pi/2$, it must descend through $\pi/2$ at a higher energy. As

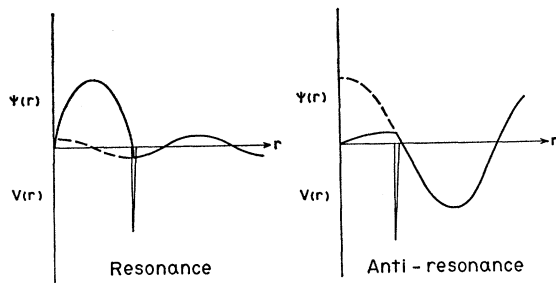


FIG. 8. Wave functions for a highly reflecting potential ditch, at resonance and at antiresonance. The phase shift is approximately $+\pi/2$ in both cases.

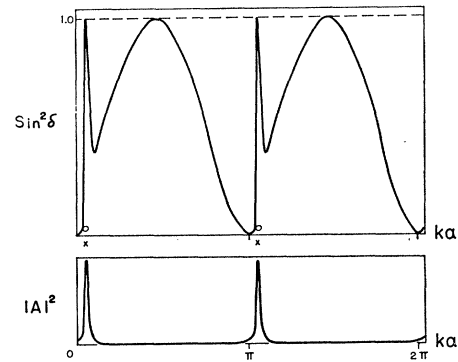


FIG. 9. $\text{Sin}^2\delta(k)$ for the $c_0 = -7$ phase shift of Fig. 4, showing resonance and echo maxima. The pole and zero position of the S matrix are also shown, as well as the $|A|^2$ curve of Fig. 6, indicating that the internal wave function is *smallest* (antiresonance) in the echo region.

Fig. 9 shows, this gives $\text{sin}^2\delta$, which is k^2 times the partial wave cross section, a large, very broad, non-resonant maximum between each pair of resonances, located exactly at antiresonance [$ka = (n + \frac{1}{2})\pi$, where $|A|^2$ is at a minimum] for a highly reflecting barrier.⁹

Just as the Wigner-Eisenbud interpretation of $d\delta/dE$ ¹⁰ implies that the energy widths of the resonance maxima in the cross section measure (inversely) the time delay of a wave packet (or the lifetime of the associated state) scattering at resonance, it equally implies that the widths of the antiresonance maxima measure the time *advance* of a packet scattering at that energy. These antiresonances are a well-known aspect of the scattering of light by dielectric spheres¹¹; they also occur in energy-averaged neutron-nucleus total cross sections, where they have variously been called "Ramsauer maxima",³ "echoes"¹⁴ and giant resonances.

For comparison, Fig. 10 shows the scattering properties of a strongly repulsive, *energy-independent* delta-function potential. Because the reflectivity of this barrier decreases with increasing energy, the $\rho\lambda$ -circle of Fig. 7 becomes a decreasing spiral, and the oscillations in $\delta(k)$ damp out as the energy increases. The resonance maxima in the internal wave amplitude (which persist even when the phase shift no longer oscillates through -90°) of course broaden with increasing energy.

Incidentally, it is interesting to note that if the *total* intensity $|S|^2$ of the reflected waves were measured (as, e.g., in a one-dimensional thin film interference

⁹ If the wave in the internal region had momentum K , the resonance spacing would be determined by $\Delta(Ka) = \pi$. If $K \gg k$ and the well has many bound states, $\Delta(ka) \approx (K/k) \Delta(Ka) \gg \pi$, and several antiresonance maxima will occur between resonances; whereas if $K < k$ (repulsive potential), $\Delta(ka) < \pi$ and there are no such maxima between resonances.

¹⁰ L. Eisenbud, dissertation, Princeton University, June 1948 (unpublished); E. P. Wigner, *Phys. Rev.* **98**, 145 (1955).

¹¹ See, e.g., the discussions in Refs. (5) and (6).

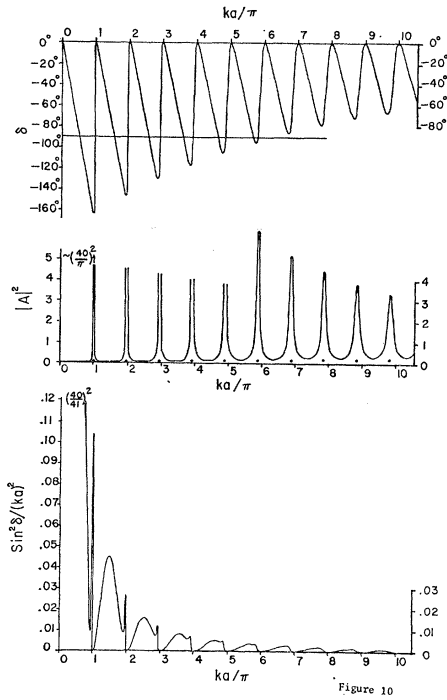


FIG. 10. Scattering characteristics of the energy-independent δ -function potential $2mV(r) = c\delta(r-a)$, with $ca = +40$. (a) Phase shift, (b) square of internal wave amplitude and (c) cross section, all as functions of the bombarding momentum. The resonance maxima are distinct from the echo maxima (which precede them in this case) only as long as the reflection at the barrier is strong enough to cause the amplitude of the phase shift oscillations to exceed 90° .

experiment), it would show no energy dependence at all, for the system absorbs nothing and $|S(k)|^2 \equiv 1$. Both resonances and antiresonances appear in the three-dimensional case only because a detector outside the incident beam measures the intensity $|1 - S|^2$ of the scattered part of the outgoing wave (which depends on the phase 2δ of S); the "1" represents the incident beam in the three-dimensional interpretation. It is basically the ability to distinguish the scattered spherical wave from the incident plane wave which makes the phase of S readily measurable in three-dimensional scattering, and so produces both the resonant and the nonresonant maxima in $\sin^2 \delta(k)$.

B. Analyticity of the S Matrix in the Case that ρ is Independent of k

The relation of the scattering resonances to the complex poles of $S(k)$ is very straightforward, for the poles occur at those complex momenta at which $[1 + \rho \exp(2ika)]$ vanishes, and it is evident from Fig. 7 that it very nearly vanishes at the real momenta corresponding to resonances, provided that the resonance widths are narrow. The pole momenta k_p , in other words, are only slightly off the real axis in this

case; since $|\rho \exp(2ik_p a)| = 1$ and in general $|\rho| < 1$, they will lie in the lower half k plane. The limiting case $\rho \rightarrow -1$ is discussed below.

From the pole condition

$$\exp(-2ik_p a) = -\rho \equiv |\rho| \exp(i\phi), \quad (10)$$

(with $\phi > 0$ for a barrier, $\phi < 0$ for a ditch) it follows that the pole positions $k_p = k_0 - i\gamma$ are given in terms of the phase and magnitude of ρ by

$$k_0 a = -\frac{1}{2}\phi \pm n\pi \quad (11a)$$

and

$$\gamma a = -\frac{1}{2} \log |\rho| \approx \frac{1}{4} |\tau|^2, \quad (11b)$$

the last approximation being valid if $|\tau| \ll 1$, i.e., low barrier transmission and narrow resonances.¹² The corresponding pole in the complex energy plane is at $E_p = k_p^2/2m = (k_0^2 - \gamma^2)/2m - ik_0\gamma/m$, so the energy width of the resonance is $\Gamma/2 = k_0\gamma/m$ and its lifetime is

$$1/\Gamma = m/2k_0\gamma \approx (2a/v_0) |\tau|^{-2}, \quad (12)$$

i.e., longer than the free-particle transit time across the sphere by the factor $1/|\tau|^2$. Incidentally, since γ depends only on $|\rho|$, the width of the resonance is the same for an attractive ($c < 0$) and a repulsive ($c > 0$) well.

The complex zeros of $S(k)$ are obtained in similar fashion and are found to be at the conjugate positions to the poles, $k_z = k_p^*$,¹³ as they must be for any elastic interaction. Consequently, the pole-zero pattern for the S matrix of a frequency-independent spherical mirror is the very simple periodic one shown in Fig. 9. If $\rho \rightarrow 0$, the poles and zeros move off to $\pm i\infty$, where they exactly cancel the essential singularity $\exp(-2ika)$, and $\delta(k) \equiv 0$. Conversely, if $\rho \rightarrow -1$, the poles and zeros move onto the real axis, where they annihilate each other in pairs, leaving only the hard-sphere term in S , $\delta = -ka$. It is only if $\frac{1}{4} |\tau| \ll \pi$ that the resonance widths will be much less than their spacings, allowing the poles to produce distinct peaks in $A(k)$ and in the cross section.

III. THE GENERAL THREE-REGION OR TWO-CHANNEL PROBLEM

Before discussing further examples, we pause briefly to work out the solution to a slight generalization of

¹² The relation $|\rho(k)|^2 + |\tau(k)|^2 = 1$, valid for real k , cannot be analytically continued into the complex k plane and so is not valid at an arbitrary pole position. However, if $|\tau| \ll 1$, the pole is very near the real axis; by continuity the relation is nearly satisfied in this case, and has been used in Eq. (11b).

¹³ The momentum dependence assumed for the potential strength has destroyed the time-reversal invariance of the Schrödinger equation and removed the customary symmetry of the pole-zero distribution about the imaginary k axis. This "doctoring" of the barrier to make it equally reflective at all energies also accounts for the fact that all resonance widths are equal. For a barrier of finite energy height E_B , e.g., those poles with $\text{Re } E_p > E_B$ would be far off the real energy axis, i.e., have very large widths and so be swamped by the "background phase", $\delta_{\text{hard}} = -ka$. The only resonances seen in the scattering cross section would occur for $E \ll E_B$, where the transmission coefficient of the barrier is low.

the above two-mirror situation, which solves a variety of problems in one fell swoop.

The generalization (Fig. 11) gives the wave a momentum K in the internal region which may be different from its external momentum k ,¹⁴ so that the transmission amplitude τ_1 across the interface from the inside out is in general different from $\tilde{\tau}_1$, the transmission amplitude from the outside in. In addition the reflection amplitude ρ_2 of the mirror or interface at $r=0$ is allowed to be different from -1 so that the waves can leak through to the $r<0$ region, giving a net flux through the system. Looked at as a one-dimensional problem, it is a simple thin film or Fabry-Perot etalon. Considered as the radial part of a three-dimensional scattering problem, the $r<0$ region is not to be ascribed geometrical reality; it is merely a familiar^{15,16} device for representing a second scattering channel, so that not all the flux incident from the right (channel 1) returns to that channel. If $-S_{11} \exp(ikr)$ is the reflected wave in channel 1 and $S_{21} \exp(-ikr)$ the wave transmitted into channel 2,

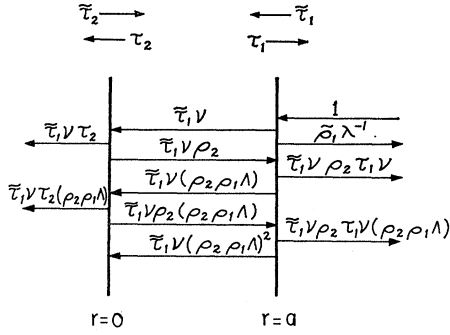


FIG. 11. Generalization of the thin film of Fig. 3 to the two-channel situation in which both interfaces are partially transparent and the internal index of refraction is different from the external. The incident wave again enters from the right (channel 1) with unit amplitude. The transmission amplitudes from the external channel regions *into* the cavity have a tilde, those from the cavity *out* to the channels do not. $\nu = (\Lambda/\lambda)^{\frac{1}{2}} = \exp[i(K-k)a]$.

¹⁴ If the dispersions in the two regions are given by the non-relativistic expressions $\tilde{p}(k) = \tilde{\omega}(k) = k^2/2m$ and $\omega(k) = K^2/2m + V$, the group velocities are $\tilde{v}_g = k/m$ and $v_g = K/m$, i.e., the "particle velocities." The phase velocities, on the other hand, $\tilde{\omega}/k$ and ω/K , are *inversely* proportional to the wave numbers, for $\omega = \tilde{\omega}$ by energy conservation. In drawing analogies between optics and potential scattering it is the phase velocities which are to be compared, since they govern both the direction of refraction and the accumulation of phase over a given path length. An attractive square well, for instance, corresponds to an optically dense object, for even though the group velocity is higher inside than out, the phase velocity is lower.

¹⁵ C. E. Porter, dissertation, Massachusetts Institute of Technology (1954).

¹⁶ W. Tobocman and D. E. Bilhorn, *Phys. Rev.* **115**, 1275 (1959). It should be recognized that this model of a two-channel situation suffers from a certain lack of generality, in that the absorption out of channel 1 is localized geometrically at the origin, $r=0$. This does not seem to strongly influence the scattering amplitude $S_{11}(k)$, whose properties are very similar, e.g., to those of a surface-absorption potential (Ref. 4).

the unitarity condition (assuming the system non-dissipative) is¹⁷

$$|S_{11}|^2 + |S_{21}|^2 = 1, \quad (13)$$

so that in general $|S_{11}|^2 < 1$, i.e., $S_{11}(k)$ [as well as $S_{21}(k)$] lies inside the unit or unitary circle.

The ρ 's at both interfaces are defined exactly as before, as are τ and $\tilde{\tau}$ at the $r=0$ interface. At $r=a$, however, we choose the phases of τ_1 and $\tilde{\tau}_1$ so that the K -to- k transmitted wave is $\tau_1 \exp[i(K-k)a] \exp(ikr)$ and the k -to- K wave is $\tilde{\tau}_1 \exp[i(K-k)a] \exp(-iKr)$. This makes all ρ 's and τ 's independent of a and preserves the form of the continuity condition $\tau = 1 + \rho$ (and $\tilde{\tau} = 1 + \tilde{\rho}$). The flux-conservation condition at either interface becomes

$$|\rho|^2 + (k/K) |\tau|^2 = 1 \quad (14a)$$

for a wave traveling from K to k , or

$$|\tilde{\rho}|^2 + (K/k) |\tilde{\tau}|^2 = 1 \quad (14b)$$

for one going from k to K . $|\rho|^2 = |\tilde{\rho}|^2 = 1 - \tau^* \tilde{\tau}$ are well-known consequences of time-reversibility, which together with (14) imply that

$$\tilde{\tau} = (k/K) \tau. \quad (15)$$

The transmission coefficient of the interface is

$$T = (k/K) |\tau|^2 = (K/k) |\tilde{\tau}|^2. \quad (16)$$

Repeating the above argument, the steady-state (traveling, not standing) wave pattern is

$$\psi_1 = \exp(-ikr) - S_{11} \exp(ikr),$$

$$\psi_{\text{int}} = A[\exp(-iKr) + \rho_2 \exp(iKr)], \quad (17)$$

and

$$\psi_2 = S_{21} \exp(-ikr),$$

with

$$S_{11}(k) = -\tilde{\rho}_1 \lambda^{-1} - [\tilde{\tau}_1 \rho_2 \tau_1 / (1 - \rho_1 \rho_2 \Lambda)] (\Lambda/\lambda), \quad (18a)$$

$$A(k) = [\tilde{\tau}_1 / (1 - \rho_1 \rho_2 \Lambda)] (\Lambda/\lambda)^{\frac{1}{2}}, \quad (18b)$$

$$S_{21}(k) = \tau_2 A(k);$$

$$\Lambda = \exp(2iKa), \quad \lambda = \exp(2ika). \quad (18c)$$

The most important general property of the solution is that its resonances, determined by the condition that $|1 - \rho_1 \rho_2 \exp(2iKa)|$ be minimized, occur at those energies which make the phase of $\rho_1 \rho_2 \exp(2iKa)$ approximately equal to 2π , provided $|\rho_1 \rho_2|$ is not varying rapidly with energy. This is the eminently

¹⁷ More generally, $|S_{11}|^2 + (k_2/k_1) |S_{21}|^2 = 1$, where k_1 and k_2 are the "channel momenta" in the two outside regions. By choosing $k_1 = k_2 = k$, our simple model makes the channel thresholds equal: at any positive energy the system both reflects and transmits.

reasonable condition that the total phase acquired by a wave in one round trip between the reflectors be 2π , so that the incident wave and that reflected internally are in phase and add constructively. In the delta-function example of Sec. II $\rho_2 = -1$, and $\rho_1 \approx -1$ if it is a good reflector. The resonance condition is then $Ka \approx \pi$, a node near the first reflector (half-wave plate). However, if ρ_1 is real and positive (as it is, e.g., for an attractive square potential well), resonance requires $\exp(2iKa) = -1$, the quarter-wave plate condition of an antinode at the first interface. Such a cavity, depending only on impedance mismatch (a single velocity change at the interface) for its reflections, leaks so badly it cannot develop substantial scattering resonances, as we discuss in detail in the following section.

Finally, we note that a consideration of the probability-conservation equation $\int \mathbf{j} \cdot d\mathbf{A} = - (d/dt) \int \rho d^3r \equiv -dP/dt$, for the case that $P(t)$, the total probability inside the cavity, decays exponentially in time [$P(t) = P_0 \exp(-t/\bar{t})$], yields the important result that the lifetime \bar{t} of an isolated narrow resonance is given in terms of the (inside-to-outside) transmission amplitudes by the two-channel generalization of Eq. (12),

$$\bar{t} \approx t_0 / (|\tau_1|^2 + |\tau_2|^2), \quad (19)$$

where $t_0 = 2a/v = 2am/k$ is the round-trip time inside the cavity at the external or free-particle velocity. Stated in other terms, Eq. (19) says that the Q value of the cavity, defined as the number of internal round trips the particle makes (at velocity K/m) in one lifetime \bar{t} , is

$$Q = (T_1 + T_2)^{-1}, \quad (20)$$

where $T = (k/K) |\tau|^2$ is the transmission coefficient of an interface.

IV. THE SQUARE WELL AND BARRIER

A. *S*-Wave "Resonances" in a Square Potential Well

A deep square potential well, $V(r) = -V_0$ for $r < a$ (a sphere of high index of refraction in optical terms), is an example of a cavity resonator whose Q value is large, but which does not have *S*-wave scattering resonances in the usual sense. By this we mean that its *S*-wave phase shift exhibits no resonance rises as a function of energy, as shown in Fig. 12, so that by the Wigner-Eisenbud interpretation of $d\delta/dE$ there are no energies at which the wave is trapped by the cavity for a significant length of time.

This is because, although the velocity change (impedance mismatch) at its surface produces the external reflection amplitude

$$\tilde{\rho} = (k - K)/(k + K), \quad (21)$$

which approaches -1 (good reflection) if $k/K \ll 1$, the

internal reflection coefficient of the same barrier is

$$\rho = (K - k)/(K + k) \quad (22)$$

which approaches $+1$ under the same conditions. Consequently, the *K*-to-*k* transmission amplitude,

$$\tau = 2K/(K + k), \quad (23)$$

approaches 2 rather than zero as $k/K \rightarrow 0$.¹⁸ According to Eq. (19) (with $\tau_2 \equiv 0$ for this one-channel potential), the lifetime of a "resonance" in this region is only half the free-particle transit time across the interaction region—and this in spite of the fact that the Q value of the cavity, Eq. (20), is very large. The number of internal reflections, $m \sim K/k$, although indeed "large," is only large enough to compensate for the higher velocity of the particle inside the potential, so that the interaction introduces no net trapping or delay time.

The high Q does imply that the system has good internal or cavity resonances, i.e., sharp maxima in the amplitude of the internal wave [Eq. (18b)],

$$|A|^2 = [1 + (K_0^2/k^2) \cos^2 Ka]^{-1}, \quad (24)$$

($K^2 = K_0^2 + k^2$ and $K_0^2 = 2mV_0$), as seen in Fig. 12. Because $\rho \sim +1$ (no phase change upon internal reflection from the surface), the system is equivalent to a quarter wave plate, with resonances [Eq. (24)] whenever

$$Ka = (n + \frac{1}{2})\pi, \quad (25)$$

the condition for an antinode at the surface, which makes the internal and external amplitudes equal. We note that if (in order to get sharp cavity resonances) $V_0 a^2$ is so chosen that $K_0 a \approx N\pi \gg \pi$,¹⁹ then the momentum spacing between the lowest resonances is $\Delta(ka) \approx f\pi(2N)^{\frac{1}{2}}$ where f is of order unity and decreases (resonances closer together) as k increases. This spacing can be many times π . Because of the high external reflection, the phase shift descends at nearly the hard-sphere rate, $\delta(k) \approx N\pi - ka$, so that it passes downward through $\pi/2$ roughly $(2N)^{\frac{1}{2}}$ times between resonances, meaning that both $\sin^2 \delta(k)$ and $\sigma(k)$ are dominated by the many Ramsauer or echo maxima which occur between each pair of resonances.

The reason that the resonances of this potential produce nothing more than small shelves on the flank of the descending background phase shift is readily understood from the well-known fact²⁰ that the poles of the *S* matrix in the range $(N\pi)^{\frac{1}{2}} \ll \text{Re}(k_p) \ll N\pi$, which are directly "below" the resonance peaks in $|A(k)|^2$, are not arbitrarily close to the real axis but rather lie nearly on the line $\text{Im}(k) = -i/a$. Because this makes

¹⁸ Of course the outgoing flux $(k/m) |\tau|^2 \rightarrow 0$, but only because the external wave comes to a halt in this limit.

¹⁹ If $(N - \frac{1}{2})\pi < K_0 a < (N + \frac{1}{2})\pi$, the potential has N bound states.

²⁰ H. M. Nussenzveig, Nucl. Phys. 11, 499 (1959).

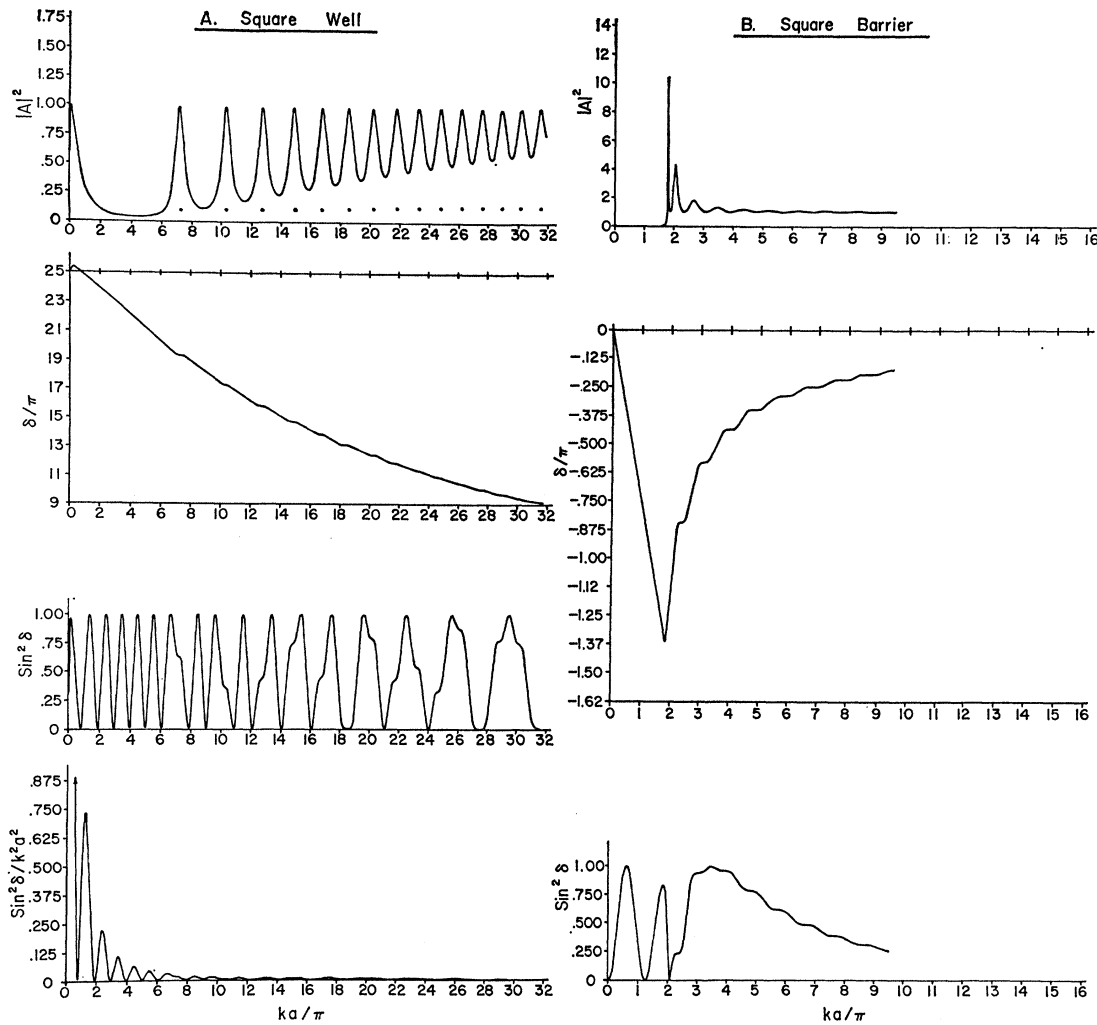


FIG. 12. (A) S -wave scattering properties of a (very deep) square potential well, $K_0 a = 25.4999 \pi$. (a) The square of the amplitude of the internal wave (for an incident wave of unit amplitude), Eq. (18b), showing its well-separated resonances in the low energy region where $k \ll K$, and their relation to the zeros of $S(k)$; the pole positions, not shown, are conjugate to the zero positions, with the exception of the one responsible for the first maximum, which is on the negative imaginary k -axis. Note that the momentum widths of the lowest resonances are all equal to $1/a$. (b) The S -wave phase shift $\delta_0(k)$. For $k \ll K_0$, it descends at very nearly the Wigner hard-sphere limit between the "resonances," which appear as small shoulders of width $\Delta(ka) \approx 1$ on this descending curve. $\delta_0(k)$ descends through 6π (six echos) between the first two resonances. (c) $\sin^2 \delta_0(k)$, showing the many echo maxima produced by the descent of the phase through $\pi/2$. The "resonances" do not appear as maxima, but merely as slight irregularities in a $\sin^2(ka)$ pattern. Note that the first maximum falls short of unity because the value of $\delta_0(k)$ at its maximum is less than $\pi/2$. (d) The S -wave total cross section, showing echo-maxima and resonance "shoulders."

(B) S -wave resonances produced by a square potential barrier. (a) Resonance maxima in $|A|^2$ at energies just above the barrier; the infinite peak exactly at the top of the barrier is not a resonance but a spurious consequence of the definition of A . Note that the poles are closer to the real k axis than in 12 (A). (b) The S -wave phase shift, showing resonant rises at the pole momenta. Because the barrier used is rather low, $K_0 a = 1.8\pi$, the resonances are broad, and the change in the background phase ($-ka$) over a resonance width is large enough to reduce the net rise in $\delta_0(k)$ considerably below π , even for the first resonance. (c) $\sin^2 \delta_0$. The strongest resonance appears as the sharp dip caused by the phase rising through $-\pi$ at $ka/\pi \approx 2$.

the resonance widths²¹ small compared to their spacings, the one-pole or Breit-Wigner approximation for $S(k)$ is valid near each resonance,

$$S(k) \approx \exp(-2ika) \left(\frac{k - k_0 - (i/a)}{k - k_0 + (i/a)} \right). \quad (26)$$

Writing $\delta(k) = -ka + \delta_0(k)$ corresponding to these two factors, and noting that $\delta_0'(k) \leq +a$, we see that $\delta'(k) \leq 0$ in this approximation, with zero slope occurring exactly at the resonance momentum k_0 . In other words, the internal reflections from the velocity change at the cavity surface do give $\delta_0(k)$ a resonant-type behavior, but one so weak it is barely able to halt the descent of the phase shift due to the nonresonant hard-sphere scattering.²² Of course, if there were a barrier (e.g., centrifugal) at the surface of the well as in Fig. 1(a), the resonances could be made much stronger, just as the transmission resonances of a Fabry-Perot etalon are sharpened by silvering its faces.

In summary, if a resonance is to produce a significant maximum in an elastic scattering cross section, its *momentum* width must be small compared to (a) the resonance momentum k_0 , (b) the spacing Δk between resonances, and (c) $1/a$, the reciprocal of the range of the interaction. The square well potential (and any other of the same general shape, such as the Woods-Saxon well of nuclear physics) is an example of an interaction whose "resonances" can satisfy (a) and (b) but not (c), corresponding to the fact that their "lifetimes" are actually shorter than the free-particle transit time across the well.²³

B. The Square Barrier

The basic reason the square well fails to develop scattering resonances is that such a cavity, although nearly impenetrable from the outside at low energy, is leaky from the inside. Exactly the reverse situation is obtained if the well is inverted to make a repulsive

²¹ Their momentum widths $1/a$ are nearly equal, but their energy widths $\Gamma \sim k_0 \gamma / m$ decrease as the resonance momentum k_0 decreases.

²² The tails of other resonances actually conspire to give $\delta(k)$ a slight maximum at $k=k_0$, but it is entirely insignificant for all resonances but the first, at which $\delta(k)$, with the help of a second pole at $-k_0 - i/a$, can rise by as much as $\pi/2$. One might well expect this lowest-energy resonance to produce a resonant rise of $\sim \pi$ in $\delta(k)$, but the boundary condition at $r=a$, $K \cot Ka = k \cot(ka + \delta)$, implies that $\delta = (n + \frac{1}{2})\pi - ka$ whenever $Ka = (n + \frac{1}{2})\pi$, so for small ka , δ is slightly less than an odd multiple of *one-half* π at resonance; a slightly more elaborate argument shows that the initial rise of $\delta(k)$ never exceeds $\pi/2$. The boundary condition also shows directly that $d\delta/dk=0$ whenever $Ka = (n + \frac{1}{2})\pi$, an alternative indication of no time delay at "resonance." Incidentally, the initial rise of $\delta(k)$ never causes a maximum in $\sigma(k)$, which falls monotonically from $k=0$ to the first echo.

²³ In one dimension, the transmission cross section (into the channel 2 region, $r < 0$) for a square well does exhibit maxima at the pole energies, for $S_{21}(k) = \tau_2(k) A(k)$ and $\tau_2(k)$ is slowly varying. Because of their very short "lifetime," it is a moot point whether they should be called resonances.

barrier, $V(r) = +V_0$, $r < a$ (optically, an air bubble in glass).

If the incident energy is just greater than the top of the barrier, it is now ρ (internal reflection) rather than $\tilde{\rho}$ which is near -1 . As discussed in Sec. III, such a cavity is a half-wave plate. The long wavelength is on the inside, and true scattering resonances can develop whenever a node occurs in the wave function near $r=a$. The phase shift and other relevant quantities are shown in Fig. 12, which indicates that the system behaves like a nearly perfect external reflector ($\delta \approx -ka$) for energies below the barrier, but exhibits rapid resonance rises in $\delta(k)$ just above the barrier. These resonances are very narrow if the barrier is high [$\text{Im}(k_p) \sim 1/K_0 a^2$],²⁰ but overlap more and more as the bombarding energy is increased above the barrier, merging into the smooth asymptotic behavior $\delta \rightarrow 0$ required at high energy by Levinson's theorem.²⁴ Although the cross section of course has echo maxima at energies below the barrier, in the resonance region the poles are too closely spaced [$\Delta(ka) < \pi$] to permit them to occur.

V. TWO-CHANNEL OR FABRY-PEROT RESONANCES

Many general properties of inelastic resonances are conveniently illustrated by the Fabry-Perot etalon or two-channel cavity of Fig. 11. In particular, since its elastic scattering cross section exhibits echo maxima, it provides an example of the way in which these nonresonant peaks can dominate the elastic (and total) cross section if the true resonances are decoupled from the entrance channel.

The simplest possible model is obtained by using a "hollow" cavity, $K=k$, whose "walls" are delta-function potential barriers with strengths proportional to k , so that both ρ_1 and ρ_2 are independent of k and lie on the circle of Fig. 2 described by $|1 + 2\rho_i| = 1$.

The partial widths for the decay of a resonance into the two channels are obtainable, e.g., from the positions of the poles of the S matrix. Since these occur at the zeros of the denominator of the S_{ij} , which according to Eq. (18) is $1 - \rho_1 \rho_2 \exp(2ika)$, they are located at

$$\text{Re}(k_p a) = -\frac{1}{2}(\phi_1 + \phi_2) \pm n\pi \quad (27a)$$

$$\begin{aligned} \text{Im}(k_p a) &= \frac{1}{2} \log |\rho_1 \rho_2| \\ &= \frac{1}{4} \log R_1 + \frac{1}{4} \log R_2 \\ &\cong -\frac{1}{4} T_1 - \frac{1}{4} T_2, \end{aligned} \quad (27b)$$

the last approximation being valid only if both $T_1 \ll 1$

²⁴ Equation (24) becomes $|A|^2 = [1 - (K_0^2/k^2) \cos^2 Ka]^{-1}$, with $K^2 = k^2 - K_0^2$ in this case. Consequently $A \rightarrow \infty$ at $k=K_0$, but this maximum is "spurious" and merely indicates that $K=0(u(r) = \text{const.} \times r$ for $r < a$) at this energy. Unless $K_0 a = N\pi$, the first resonance is at the *second* maximum in $|A|^2$.

and $T_2 \ll 1^{12}$; ϕ_i is the phase of ρ_i . Consequently, in agreement with Eq. (19), the total energy width of a narrow resonance is

$$\Gamma \approx t_0^{-1}(T_1 + T_2), \quad (28)$$

where $t_0 = 2am/k$ is the free-particle transit time across the dimensional cavity. The partial widths are consequently

$$\Gamma_i = T_i/t_0, \quad (29)$$

i.e., proportional to the transmission coefficients into the corresponding channels.

As for zeros, $S_{21}(k)$ has none and those of $S_{11}(k)$ occur at the solutions of

$$\exp(-2ik_za) = -(1 + 2\rho_1)(\rho_2/\rho_1).$$

They lie directly above the poles,²⁵ at a distance from the real k axis given by

$$\text{Im}(k_za) = \frac{1}{2} \log(\rho_2/\rho_1) \approx \frac{1}{4}(T_1 - T_2), \quad (30)$$

and so are in the upper half k plane if $\Gamma_1 > \Gamma_2$ and in the lower half if $\Gamma_1 < \Gamma_2$; if the cavity is coupled equally to the two channels, the zeros of S_{11} occur at real energies (in fact, exactly the resonance energies). Note that $E_z - E_p \cong i\Gamma_1$, the entrance channel width.

These properties agree, of course, with the Breit-Wigner approximation for S_{11} near a resonance,

$$\begin{aligned} S_{11}(E) &= \exp(2i\phi) \left(1 - i \frac{\Gamma_1}{E - E_0 + i(\Gamma/2)} \right) \\ &= \exp(2i\phi) \left(\frac{E - E_0 + i[(\Gamma/2) - \Gamma_1]}{E - E_0 + i(\Gamma/2)} \right), \end{aligned} \quad (31)$$

whose zero and pole have the same real part E_0 and are separated by the energy $i\Gamma_1$; the zero is on the real axis if the resonance is half in the entrance channel, $\Gamma_1 = \Gamma/2$. (ϕ is the slowly varying background phase.)

Alternatively the B-W approximation can be written in terms of the resonant part of the eigenphase concerned, defined by the pole parameters according to

$$\tan \delta_r(E) = \Gamma/2(E_0 - E). \quad (32)$$

As a function of δ_r , the Breit-Wigner expression is

$$S_{\alpha\beta} = \exp(2i\phi) \{ \delta_{\alpha\beta} + (\Gamma_\alpha \Gamma_\beta)^{1/2} / \Gamma [\exp(2i\delta_r) - 1] \}. \quad (33)$$

Since $\delta_r(E)$ rises from zero to π over roughly the energy interval 2Γ , Eq. (33) indicates that the complex

²⁵ This is a general property of narrow resonances; the fact that it holds for all resonances in this case is a peculiarity of the model.

number $S_{\alpha\beta}(E)$ travels around a circle of radius $(\Gamma_\alpha \Gamma_\beta)^{1/2} / \Gamma$ ($\leq \frac{1}{2}$ for $\alpha \neq \beta$) over the same energy range. At antiresonance, $\delta_r = 0$ or π , this circle passes through the origin in the $S_{\alpha\beta}$ plane for off-diagonal elements, and is tangent to the unitary circle {at the point $\exp[2i\phi(E_0)]$ } for diagonal S -matrix elements. In $S_{\alpha\alpha}$ it coincides with the unitary circle for an elastic resonance, and shrinks in size as the entrance channel is decoupled from the resonance.

These properties are clearly illustrated by Figs. 13 and 14, which show the complex trajectories followed by the S -matrix elements of Eq. (18) as the bombarding energy is varied, as well as the corresponding elastic (1→1 reflection) and inelastic (1→2 transmission) cross sections. Because ρ_1 and ρ_2 are independent of k in this model, $S_{11}(k)$ and $S_{21}(k)$ are again periodic, so their complex trajectories close after one period.

In Fig. 13 the entrance channel barrier is taken to be highly impenetrable ($T_1 = 0.1$), and the three columns correspond to different choices for the "inelastic" barrier.²⁶ More exactly, we have chosen $\text{Im} \rho_1 > 0$ (ditch) and $\text{Im} \rho_2 < 0$ (barrier). This corresponds to the boundary conditions of a Fabry-Perot etalon and makes the resonances occur exactly at $ka = n\pi$ in the symmetric case, $\Gamma_1 = \Gamma_2$ ($\rho_1 = \rho_2^*$ or $\phi_1 = -\phi_2$).

In Fig. 13(1) both barriers are highly reflecting, the second even more so than the first, so the resonances are narrow and have their widths predominantly in channel 1. $S_{11}(k)$ shows a nearly elastic resonance circle [rapidly increasing phase, caused by the second term of Eq. (18b)] followed by an echo circle [slowly decreasing phase, due to the first term of Eq. (18b)], while $S_{21}(k)$ (which would vanish identically if Γ_2 were zero) has only a small resonance circle. The elastic cross section, $|1 - S_{11}|^2$, has alternating resonance and echo maxima as a function of energy, while the reaction cross section or 1→2 transmission coefficient $|S_{21}|^2 = 1 - |S_{11}|^2$ shows small resonance peaks but of course no echoes, since they are caused by the phase of S_{11} , to which the transmission cross section is insensitive.

Figure 13(2) shows a good Fabry-Perot etalon or band-pass filter. Because the cavity is coupled equally to both channels, S_{11} vanishes (and $|S_{21}| = 1$) exactly at resonance, so the transmission is perfect, and nothing is reflected into the entrance channel.²⁷ Furthermore, both partial widths are small so the transmission peaks are narrow and well-separated in energy. Since the resonance circle in S_{11} has shrunk to half its elastic size, however, the resonance peaks in the elastic cross

²⁶ We have chosen the case of fixed Γ_1 and increasing Γ_2 as an illustration because it corresponds closely to the way in which the partial widths predicted by an optical potential vary as the absorptive part of the potential is increased from zero.

²⁷ The scattered intensity in channel 1, $|1 - S_{11}|^2$, is of course not zero in this case, but in fact equal to the intensity in channel 2. Cf. the comparison of the one-dimensional and three-dimensional interpretations at the end of Sec. IIIA.

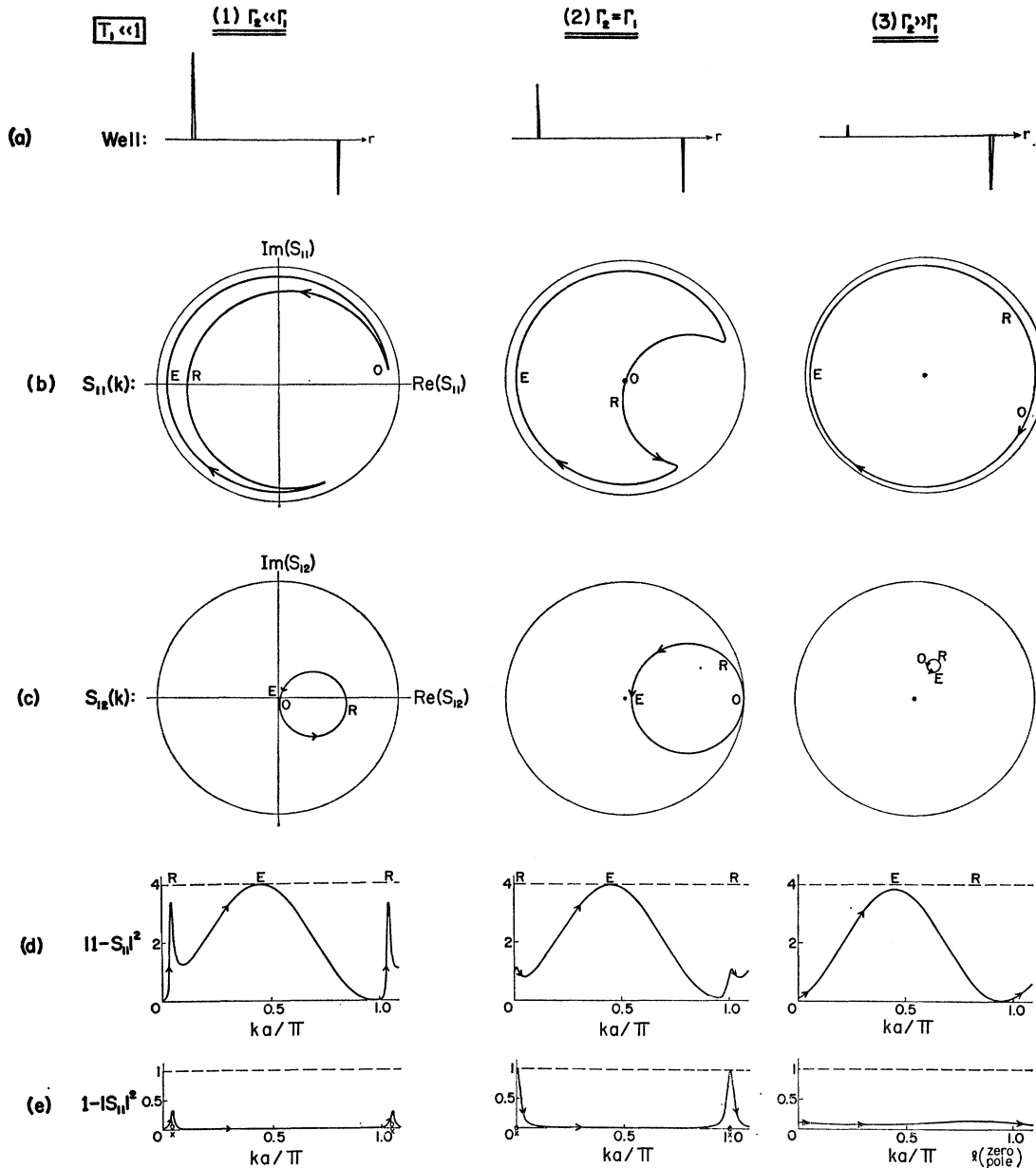


FIG. 13. Two-channel scattering properties of a Fabry-Perot etalon with a strongly silvered front surface ($T_1=0.1$); both the front and rear transmission coefficients are taken frequency-independent. In column (1), $T_2=0.01$ and the resonance is predominantly in channel 1; in column (2) ($T_2=T_1$) it is equally coupled to both; and in column (3) ($T_2=0.97$) it is predominantly in channel 2. Row (a) indicates schematically the relative strengths of the delta function potentials at the faces of the device for these three cases. (b) The path followed in the complex plane by $S_{11}(k)$ as the energy increases. The resonance and echo energies are indicated along the trajectories; in addition the points at which $ka/\pi = 0, 0.03$ and 0.3 are marked by (0) and the two arrowheads, which are repeated on the other diagrams as well. In column (3), "R" indicates the point at which $k = \text{Re}(k_p)$, where the weak maximum occurs in the reaction cross section. The resonance circle appears clearly in columns (1) and (2), but has vanished from S_{11} completely in column (3); it would of course appear in S_{22} . (c) The S_{22} trajectory, showing a resonance circle which is largest in the case of equal coupling to the two channels. (d) The S -wave elastic scattering cross section (times k^2), indicating how the narrow resonance maxima disappear as the partial width is transferred out of the entrance channel; the nonresonant echo is largely unaffected. (e) The reaction or transmission cross section [which is also proportional to $|A|^2$, Eq. (18c)], showing resonance maxima which broaden as the poles and zeros (also indicated) move downward. Perfect transmission is possible only when $\Gamma_1 = \Gamma_2$.

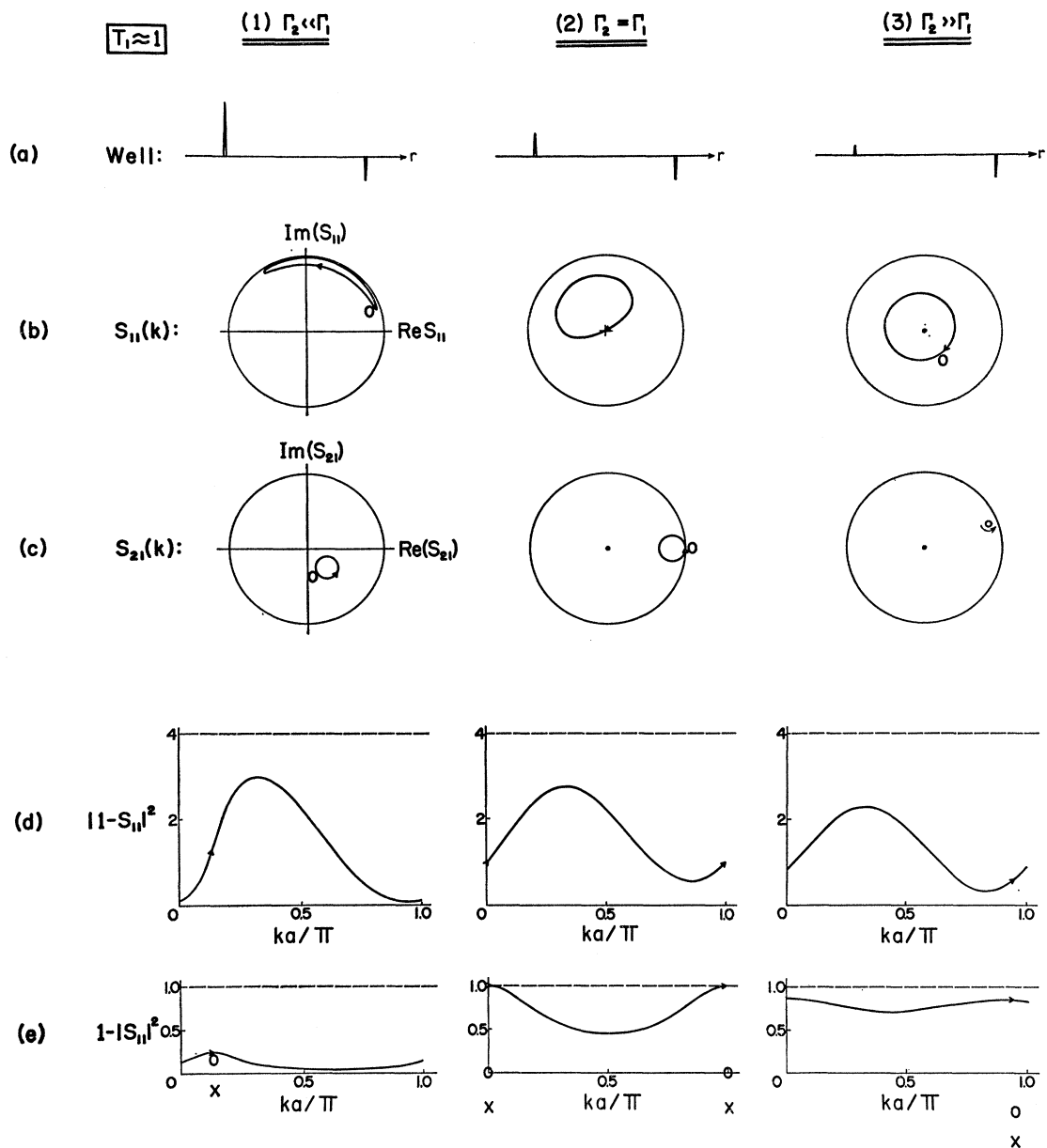


FIG. 14. Same as Fig. 12(A) but with the front surface of the etalon weakly silvered ($T_1=0.8$). Since the cavity leaks through the entrance channel, it cannot develop narrow resonances for any value of Γ_2 . The arrowhead on all diagrams marks the pole momentum, $k = \text{Re}(k_p)$, and $k=0$ is indicated by 0.

section are down by a factor of 4; the nonresonant echo maxima are not greatly affected by the opening of the second channel.

In Fig. 13(3) the cavity is allowed to leak strongly into channel 2. This broadens the transmission peaks until they overlap, and moves the resonances so heavily into channel 2 that they are in effect decoupled

from channel 1 altogether ($\Gamma_1/\Gamma \ll 1$), with the consequence that S_{11} executes almost pure echo circles. [$\rho_2 \rightarrow 0$ removes the resonance term of S_{11} in Eq. (18a), leaving $S_{11}(k) = -\rho_1 \exp(-2ika) \approx \exp(-2ika)$]. The only significant structure remaining in the energy dependence of the elastic (and total) cross section is provided by the echoes, i.e., the system scatters

almost exactly like an impenetrable (hence nearly elastic) sphere.²⁸

Figure 14 shows the less interesting situation in which the entrance-channel barrier is very transparent ($T_1=0.8$), so that good resonances cannot develop no matter what Γ_2 is. In 14(1), Γ_2 is chosen practically zero to give nearly elastic scattering in channel 1, but because of its leaky barrier the phase shift only rises a few degrees before falling again, giving only the weakest indication of "resonance" maxima in the cross sections. Figure 14(2), with equal coupling to the two channels, is again a Fabry-Perot etalon, but this time with only weakly silvered faces, so both its transmission and its reflection resonances overlap. In 14(3) both widths are large, but the "resonance" has been shifted so predominantly into channel 2 that S_{11} shows only echo circles. In this case the entrance barrier is only weakly reflecting, so $S_{11} \approx \rho_1 \exp(-2ika)$, with $|\rho_1| \ll 1$, and even the echo circle is small.

Finally, we mention an alternative model for inelastic resonances which is the exact analogue of the optical model, namely the single delta-function potential of Fig. 1(b), with a complex coefficient, $c=c_1+ic_2$. For appropriate choices of c_2/c_1 , its cross sections look much like those of Figs. 13 and 14, but the pole-zero structure of the $S_{11}(k)$ it predicts is somewhat more bizarre. ρ lies inside the circle of Fig. 2 if $c_2 < 0$ (absorptive potential) and on the real axis if $c_1=0$. $\text{Re}(k_z) = \text{Re}(k_p)$ only if $c_2=0$ or $c_1=0$, in this case, and for c_2 large enough [$(c_2/k)^2 > 2 + (c_1/k)^2$ in the case that c is chosen proportional to k], the zero lies below the pole in the k plane! Needless to say, a cavity this inelastic has no significant resonances. Equation (4) shows that $\rho \rightarrow -1$ as $c \rightarrow \infty$ in *any* complex direction, corresponding to elastic hard-sphere scattering, with the zeros and poles of S_{11} cancelling each other in pairs on the real k axis; even a purely

imaginary δ -function potential is a perfect reflector if it is strong enough.

SUMMARY

The principal unifying thread which has emerged to connect these diverse examples of resonating systems is the so-called background phase, whose influence on elastic cross sections is seen to be disconcertingly great when the resonances are not sufficiently narrow. In the present models, whose interactions are concentrated on a spherical shell, it is evident from the ray-tracing technique that this background phase arises principally from the instantaneous ("direct interaction") reflection of the incident wave from the surface of the target; this reflection causes the largest spatial advance in the scattered wave and so the largest negative contribution ($-a$) to the slope of $\delta(k)$. Although a background phase of this nature will not appear if the interaction is too "soft" to define a target surface (e.g., the Coulomb potential), it is to be expected for any "finite-ranged" potential [$r^n V(r) \rightarrow 0$ at large r , for any n]. A wide variety of nuclear reactions, e.g., have shown that the round-edged nucleon-nucleus potential (with its Yukawa tail) produces a hard-sphere background phase, $\delta_B(k) \approx -kR$, with R approximately equal to the nuclear "radius."

Although it can only be of major significance far from sharp resonances, this decreasing component of the phase shift not only eliminates resonant peaks from the S -wave scattering by a square potential well altogether, but in many instances even adds non-resonant peaks of its own to elastic cross sections. Reaction cross sections, on the other hand, are insensitive to the phase of the corresponding S -matrix element, and so are never plagued by confusing background-phase effects.

ACKNOWLEDGMENTS

Thanks are due to Mrs. Mary Menzel and Dr. H. M. Ruppel of the Los Alamos Scientific Laboratory, and to William Romo of the University of Wisconsin for their able assistance with the computations shown in the figures.

²⁸ It is worth noting that although $T_2 \approx 1$ in the particular example used in Fig. 13(3), the absolute magnitude of T_2 is not significant. Only the ratio T_2/T_1 counts, and the same degree of resonance decoupling from channel 1 could have been achieved, e.g., by the choice of $T_1=0.01$ and $T_2=0.1$ —i.e., with only very weak coupling to channel 2.